

Optimum Design of Corrugated Board under Buckling Constraints

Daxner, T., Flatscher, T., and Rammerstorfer, F.G.

Institute of Lightweight Design and Structural Biomechanics,
Vienna University of Technology, Gusshausstrasse 27-29/E317, A-1040 Vienna.
(Email: daxner@ilsb.tuwien.ac.at, flatscher@ilsb.tuwien.ac.at, ra@ilsb.tuwien.ac.at)

Abstract

Corrugated paper is produced in large volumes for packaging purposes, an application which places high demands on the structural stability of the employed corrugated board containers. This is taken into account in the optimization procedure for reducing the area-specific weight of corrugated board which is presented in this paper.

For predicting effective properties of corrugated board designs, the geometry of the board is discretized by finite shell elements, and a periodic unit cell model, which contains a minimum of one full wave of the flute, is generated. By application of appropriate periodicity boundary conditions, the effective mechanical behavior of a theoretically infinite board can be predicted within the limits of linear shell theory. Furthermore, local loss of stability can also be calculated. It is possible to embed this model into an optimization procedure which attempts to reduce the area-specific weight of the board by modifying the governing geometrical parameters while enforcing the stiffness and buckling strength constraints. It has to be noted that the calculation of critical loads with respect to local buckling involves a minimization scheme within this optimization loop in order to find the critical buckling wavelength and adjust the unit cell size accordingly.

We apply the proposed optimization scheme to a specific kind of corrugated board in order to determine if there is potential for weight-reduction. The optimization scheme gives a set of parameters which describes a new design of corrugated paper with the same buckling strength, but an area-specific weight that is reduced by more than 18% with respect to the original design. The improved corrugated board shows simultaneous buckling of fluting and liners under a compressive membrane load along the generatrix of the flute.

Keywords: corrugated board, optimization, buckling, finite element method.

1. Introduction

Corrugated board is used in significant quantities for packaging purposes, where its good weight-specific stiffness and strength properties are exploited in the construction of boxes and containers for the protection and the transport of goods. Since corrugated board is a sandwich structure consisting of a wavy core called flute and face sheets called liners it is prone to buckling both on the global level of the box walls and the local level of liner and/or flute. In the following, a brief overview over relevant literature on the buckling behavior of corrugated board will be given.

In-plane loading of corrugated board will, in general, be of biaxial nature. Thus, it is important to consider the interaction of simultaneous loads acting in different in-plane directions. Patel *et al.* [1] contribute to this subject by loading cylindrical shells made from corrugated board under combinations of axial compression, torque and external pressure, thereby deriving experimental failure envelopes under interacting global loads. In view of the need to predict the failure of corrugated board under biaxial loading, a failure criterion for the board liners has been proposed in [2], taking into account both the strength of the material itself and its structural stability. This paper is put into a wider context in the doctoral thesis of Nyman [3].

The onset of global buckling in corrugated board is certainly influenced by the kinematic boundary conditions, which have to be implemented carefully in experiments and simulations alike. Allanson and Svärd [4] show full-scale finite element simulations for a square corrugated board under uniaxial loading and simple supports on all edges. Favorable agreement with experimental results is demonstrated with respect to predicted force-displacement relationships and the onset of failure.

For practical packaging applications the strength and stability of boxes made from corrugated board are of great importance. Stacking boxes on top of each other places the highest load on the box at the bottom, which has to possess sufficient box compression strength for withstanding this load without collapsing. A lasting contribution for the design of corrugated board containers is the design formula proposed by McKee [5]. Attempts for a more accurate prediction of the compression strength of corrugated containers comprise finite element simulations of the whole box (including closure fins) using shell elements that exhibit the same effective orthotropic stiffness as the actual corrugated board, compare [6] and [7]. In [6] a good agreement between simulation results and experimental data was obtained for both the initial buckling load and the limit load, the latter being approximately twice as high as the former for the considered type of box.

Different modes of instability can be triggered by compression in thickness direction of the corrugated board. The response of corrugated board to a crushing deformation in face normal direction is governed by snap-through buckling and progressive self-contact leading to nearly complete densification of the board, see [8] for a corresponding finite element study including effects of imperfections as well as experimental results.

In this paper, we discuss methods of improving corrugated paper designs by applying numerical sizing optimization methods for the reduction of the area-specific weight of the board while maintaining a required buckling strength both on the level of local buckling of liners and fluting and on the level of global buckling of whole plates made from corrugated board, see also [9].

It has to be pointed out, that the terms ‘optimization’ and ‘optimum’ used in this paper do only apply in a local sense, because the non-linear nature of the optimization problem does not allow for the guaranteed prediction of a global optimum.

2. Method

2.1 Problem Description

The objective of this study was the development of a framework for the minimization of the area-specific weight of corrugated board in the presence of local and global stability constraints. The study is concerned exclusively with single wall corrugated boards as shown in Fig. 1. This type of corrugated board consists of one ply of fluted paper which is glued between two plies of paper or cardboard.

Figure 1 shows the geometrical parameters of the unit cell model for corrugated board. The overall dimensions are described by Fig. 1 (*left*), where l_{uc} denotes the length of the unit cell in 1-direction, b_{uc} marks the width of the unit cell, which is equal to the wavelength b_{wl} of the liner in the presented example, and h_{uc} describes the overall thickness of the finite element model as the distance between the reference planes of the liner shell elements. Note, that this thickness does not correspond to the actual overall thickness of the corrugated board. A detailed description of the geometrical parameters of the individual paper sheets can be found in Fig. 1 (*right*), which represents a cross-section of the corrugated board normal to the flute generatrix. The thickness of the flute is defined by t_F , while the thickness of the liners is given by t_L . The flute is represented by a sinus function. The shell elements representing the liners are shown to have an offset of h_o from the reference surface, on which the finite element nodes are defined. This simplifies the model generation, because the kinematic coupling between flute and liners is established by sharing the same FE nodes, without changing the effective mechanical properties. Of course this approach implies perfect bonding between fluting and liners. An additional parameter b_b , which can be used to define a finite bonding region, is set to zero for this study, $b_b \equiv 0$.

For the definition of a reference configuration, from which the optimization procedure can be started, geometrical parameters and material data for actual corrugated board has been extracted from [1]. Two cases have been examined: (a) corrugated board made from a fictitious, isotropic, paper-like material with $E = 8000$ MPa and $\nu = 0.3$, for which the geometrical parameters are given as $b_{wl} = 7.2$ mm, $h_{uc} = 3.6$ mm, and $t_F = t_L = 0.2$ mm, as well as (b) corrugated board with orthotropic paper material parameters as defined in Table 1. The directions l - q - t , which are local to the shell elements, are defined as in-plane/parallel to the generatrix, in-plane/normal to the generatrix, and out-of-plane with respect to the individual elements, respectively. The density of paper was assumed to be $\rho = 805$ kg/m³ for both cases.

The reference design was evaluated in terms of the critical compressive load in the longitudinal, 1-

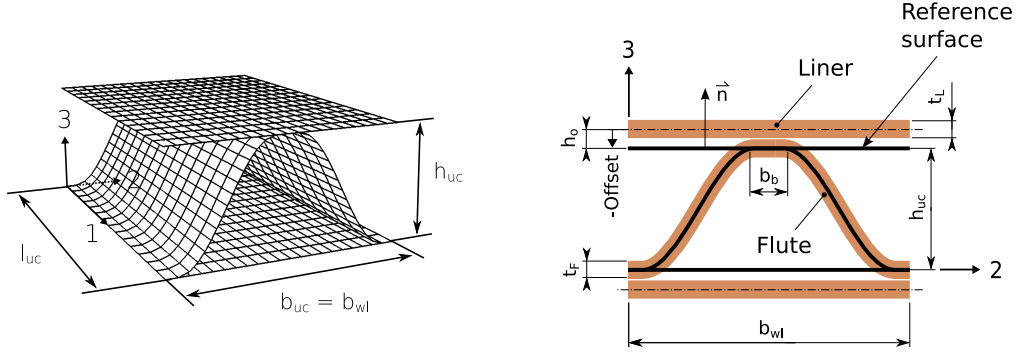


Figure 1: Principal dimensions of a corrugated board unit cell (*left*) and correlation of shell reference surfaces and shell middle surfaces (*right*) in the finite shell element model.

Table 1: Geometrical parameters for the original, unoptimized corrugated board along with orthotropic material data; based on data for actual corrugated board published in [1].

$b_{wl} = 7.2$ mm	Liner	Flute	
$h_{uc} = 3.6$ mm	E_l	3010	2260 MPa
$t_L = 0.231$ mm	E_q	8220	5270 MPa
$t_F = 0.252$ mm	ν_{ql}	0.17	0.17 -
$\beta_b = 0.0$	G_{ql}	1920	1340 MPa
$\bar{A} = 0.8302$ mm	G_{lt}	45	45 MPa
	G_{qt}	45	45 MPa

direction, $|N_{11,0}^*|$, that leads to local buckling and in terms of its effective bending stiffness $B_{1,0}$ about the transverse 2-direction. Furthermore, the width-specific cross-sectional area \bar{A} was calculated according to:

$$\bar{A} = \frac{2b_{wl}t_L + L_F t_F}{b_{wl}} \quad (1)$$

where L_F denotes the running length of flute paper for a full sinusoidal wave of the fluting, compare Fig. 1. Starting from the reference geometry, we now pose the following constrained optimization problem:

Minimize the weight per unit area of the corrugated board (i.e., \bar{A}) by a variation of b_{wl} , h_{uc} , t_L , and t_F , respectively, while retaining at least the same strength of the original design with respect to local buckling under compression in 1-direction, as well as retaining at least the same stiffness for bending about the 2-direction (for preventing global loss of stability.)

A semi-analytical and a purely numerical optimization approach will be proposed in Sections 2.2 and 2.3, respectively. Both depend, albeit to varying degrees, on a finite element unit cell model for corrugated board that shall be described in the following.

2.2 Finite Element Unit Cell Model

In order to calculate effective properties of corrugated board, such as effective stiffness or critical compressive membrane forces, finite element unit cell models as shown in Figure 1 (*left*) were set up in the general purpose finite element code *ABAQUS* (www.abaqus.com).

The unit cell concept can be outlined only briefly here; by means of appropriate kinematic boundary conditions it is possible to predict the effective mechanical behavior of spatially periodic structures while only modelling a small, geometrically representative building block of the structure, the so-called *unit cell*. In our case, the boundary conditions were chosen such that the unit cell had all macroscopic degrees-of-freedom that are provided by classical Kirchhoff/Love shell theory, meaning that no overall

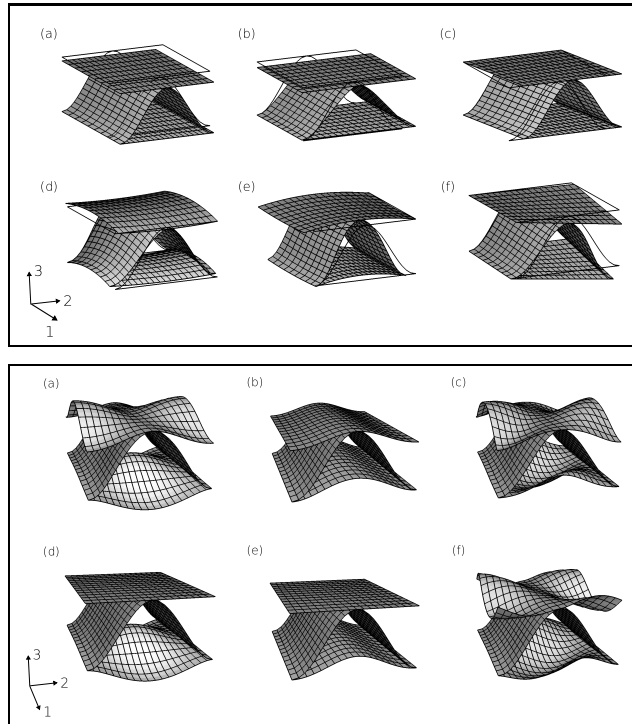


Figure 2: Unit load cases (*top box*) and corresponding buckling modes (*bottom box*) for uniaxial loading in 1-direction (a), uniaxial loading in 2-direction (b), in-plane shear loading (c), bending about the 2-axis (d), bending about the 1-axis (e), and twisting (f).

transverse shear deformation is taken into account. However, an overall thickness reduction of the board under loading can be simulated as well as local deformations in the board cross-sections.

The macroscopic deformation of the unit-cell was super-imposed on a field of microscopic deformations that was periodic in 1 and 2 direction, respectively, from one side of the unit cell to the other. By appropriate processing of (micromechanical) nodal forces, effective macromechanical membrane forces and sectional moments can be obtained. The details of this procedure are beyond the scope of this paper. They can, however, readily be found in [10]. Furthermore, the basic deformation modes of the described unit cell models are presented in Fig. 2 (*top*): mode (a) corresponds to uniaxial tension in longitudinal 1 direction, mode (b) is caused by uniaxial tension in transverse 2 direction, mode (c) is the result of in-plane shear forces. Modes (d) and (e) are predicted for bending about the transverse 2 direction, and the longitudinal 1 direction, respectively. The deformed configuration (f) in Fig. 2 (*top*) reflects the effects of a macroscopic twisting moment.

For those macroscopic load cases, that do not involve in-plane shear deformations of the liners, the corresponding critical loads with respect to local buckling of the flute and/or the liners can be calculated in a straightforward manner by solving the corresponding linear buckling eigenvalue problem with *ABAQUS*. The corresponding buckling modes are presented in Fig. 2 (*bottom*) with the same load case identifiers (a,b,d,e) as described in the previous paragraph. In this figure, the periodic nature of the microscopic displacements is particularly obvious and demonstrates the appropriate definition of the periodic boundary conditions. Shear dominated buckling modes can only be predicted qualitatively with the present unit cell model as shown in Fig. 2 (c) and (f).

Flute and liners were discretized with 8-node, bi-quadratic finite shell elements with reduced integration. The mesh refinement had to be a sensible compromise between numerical accuracy and numerical effort, because each optimization procedure consisted of hundreds of individual finite element analyses. A convergence study was performed and a fixed ratio of approximately 0.075 between the element length in the 2-3-plane and the spatial distance between diagonally adjacent bonding points was found to give

reliable predictions for the expected flute curvatures in connection with an element length in 1-direction that was twice as large as the aforementioned length.

2.3 Semi-Analytical Optimization Approach

The optimization problem under consideration involves four free geometrical parameters (b_{wl} , h_{uc} , t_L , and t_F), the calculation of the effective bending stiffness about the transverse 2-axis, and the calculation of critical compressive membrane loads $|N_{11}^*|$ that lead to local buckling in the sandwich compound.

For the most general case, that includes orthotropic material data and allows for an interaction of fluting and liners during buckling, an analytical treatment of the buckling problem certainly becomes unfeasible. The treatment of the buckling problem can, however, be simplified by assuming isotropic material behavior and by the assumption that there is no interaction between the buckling mechanisms of liners and fluting. For this simplified system it is possible to give reasonable estimates for the buckling stress $\sigma_{11,L}^*$ of the liners and the buckling stress $\sigma_{11,F}^*$ of the fluting, respectively, the loading being in-plane compression in the longitudinal 1-direction. The optimization problem can then be expressed, e.g., by postulating optimal properties for simultaneous buckling of fluting and liners:

$$\sigma_{11,L}^* = \sigma_{11,F}^* \quad (2)$$

and minimizing \bar{A} accordingly. The required bending stiffness $B_1 \geq B_{1,0}$ has to be introduced as an additional constraint.

This approach requires estimates for the buckling stresses of liners and fluting. The buckling stress $\sigma_{11,L}^*$ of the liners can be described rather conveniently by the following formula used for the prediction of elastic buckling stresses for rectangular, isotropic plates:

$$\sigma_{11,L}^* = k E \left(\frac{t_L}{b_{wl} - b_b} \right)^2 \quad (3)$$

The factor k depends on the Poisson's ratio ν of the material, on the length-to-width ratio of the plate, on the kinematic boundary conditions, and on the type of the loading. Treating the liners as infinitely long plates, that are clamped along their edges, and loaded under compression in their longitudinal direction gives $k = 6.4$ for $\nu = 0.3$. As long as the buckling mode corresponds to the kinematic assumptions, i.e., as long as it is symmetric with respect to the bonding line between fluting and liners, this equation gives a fairly accurate prediction of the respective buckling stress.

The prediction of the buckling stress $\sigma_{11,F}^*$ of the fluting was more involved, as no closed-form solution was available. It was decided to approximate the buckling stress $\sigma_{11,F}^* = \sigma_{11,F}^*(h_{uc}, b_{wl}, t_F, b_b, E)$ for the special case $b_b = 0$ by a fitting function that was similar in structure to Eq. (3). This fitting function was defined as:

$$\sigma_{11,F}^* \approx \tilde{k}_F E \left(\frac{t_F}{\tilde{b}_F} \right)^2 \quad (4)$$

With the dimensionless geometrical parameters $\bar{b}_F = (b_{wl} - 2b_b)/(2t_F)$ and $\bar{h}_F = h_{uc}/t_F$ the following fitting functions were found to give good results for the equivalent buckling factor \tilde{k}_F and the equivalent plate width \tilde{b}_F without introducing too many fitting parameters:

$$\tilde{k}_F = \kappa_{00} + \kappa_{10} \bar{b}_F + \kappa_{20} \bar{b}_F^2 + \kappa_{01} \bar{h}_F + \kappa_{02} \bar{h}_F^2 \quad (5)$$

$$\tilde{b}_F = \left(1 + \beta_1 \left[\frac{\bar{b}_F}{\bar{h}_F} \right]^{0.5} + \beta_2 \left[\frac{\bar{b}_F}{\bar{h}_F} \right] \right) \sqrt{\bar{b}_F^2 + \bar{h}_F^2} \quad (6)$$

The seven unknown fitting parameters κ_{ij} and β_i were consequently determined by fitting the values of Eq. (4) to sample buckling stresses predicted by means of a finite element unit cell model of the fluting, see Fig. 3. The least-squares fitting function 'FindFit' of the mathematical software *Mathematica* (www.wolfram.com) was used.

With appropriate analytical expressions for $\sigma_{11,L}^*$ and $\sigma_{11,F}^*$ being available in the form of Eqs. (3) and (4), respectively, an optimization problem $\bar{A}_{opt} = \min(\bar{A})$ can be formulated under the inequality

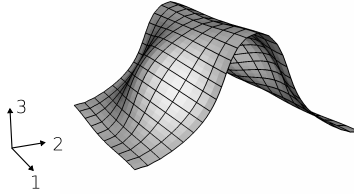


Figure 3: Predicted buckling mode for local buckling of the fluting (without liners) under compressive loading along the generatrix of the flute (1-direction).

constraints $\sigma_{11,L}^* \geq |N_{11}^*|/\bar{A}_{\text{opt}}$, $\sigma_{11,F}^* \geq |N_{11}^*|/\bar{A}_{\text{opt}}$, $B_1 \geq B_{1,0}$, and $b_{w1}, h_{uc}, t_L, t_F \geq 0$. This optimization problem was solved numerically with the function ‘NMinimize’ of *Mathematica*, which implements, among others, a Downhill-Simplex method and a genetic algorithm, both of which were used in this study and gave identical results, see Section 3.

2.4 Numerical Optimization Approach

The semi-analytical approach discussed above contains a number of simplifications that are not necessary if a suitable optimization algorithm is wrapped around a finite element model that performs the necessary mechanical calculations with arbitrarily high accuracy for general settings.

Specifically, the prediction of the critical compressive membrane force in longitudinal direction $|N_{11}^*|$ can be performed with a finite element unit cell model such as the one described in Section 2.2 and the linear buckling eigenvalue prediction capabilities of *ABAQUS*. This, however, implies the introduction of an additional geometrical variable, that so far did not play a role, namely the unit cell length l_{uc} . The buckling mode shape is influenced by this parameter, because the length of the unit cell, in connection with the periodic boundary conditions in the longitudinal direction, imposes kinematic constraints on the unit cell model that would not be present in an ‘ideal’ model of infinite length. Such an infinite, or even a semi-infinite model is not feasible numerically, and a strategy is necessary for predicting the (theoretical) buckling strength of the infinite board strip with a finite-size model.

This poses an optimization problem by itself, namely the minimization of $|N_{11}^*|$ by variation of l_{uc} for a given set of parameters h_{uc} , b_{w1} , t_F , and b_b . Figure 4 presents the dependency of the longitudinal buckling membrane force $|N_{11}^*|$ on the length of the unit cell l_{uc} in form of a diagram. The corresponding corrugated board data was the one described for the isotropic reference configuration. For $l_{uc} \rightarrow 0$ the buckling force rises to infinity, because this equals $b \rightarrow 0$ in the term $(t/b)^2 \propto \sigma^*$ that is a factor of proportionality for the buckling stress σ^* of a rectangular plate under uniaxial compression. For $l_{uc} \rightarrow 10$ mm the critical membrane force begins to drop and reaches a local minimum at $l_{uc} \approx 10$ mm. This local minimum represents the natural buckling mode of the infinite strip very well insofar, as the unit cell length is equal to the theoretical wavelength of the wavy buckling pattern in the infinite setting. As soon as the unit cell length is increased further, the buckling force rises again until $l_{uc} \approx 15$ mm, and then drops again as l_{uc} approaches ≈ 20 mm. Here, a second local minimum is visible, since the unit cell now is able to accommodate two full buckle wavelengths, compare the corresponding insert image in Fig. 4. This pattern can be repeated for increasing unit cell lengths, as the dashed line in Fig. 4 indicates. If the unit cell is long enough, small variations of the unit cell length do not play a significant role any more, because the actual buckling wavelength will be close to the theoretical wavelength no matter what the actual length of the unit cell is.

Both the solid line and the dashed line in Fig. 4 drop off at certain large values of l_{uc} . The reason for this unexpected behavior is that the local buckling mode becomes energetically less favorable than a global buckling mode reminiscent of Euler beam buckling. This is indicated by the inset pictures at the right side of Fig. 4, which show one buckling half-wave for the lowest eigenvalue (solid line) and two buckling half-waves for the next-to-lowest eigenvalue (dashed line). The physical relevance of these results is questionable, because for the prediction of the global buckling of corrugated board as a plate it is certainly necessary to define the kinematic boundary conditions in a manner that is less artificial than the one inherent in the periodic boundary conditions. Recall, that global buckling is represented

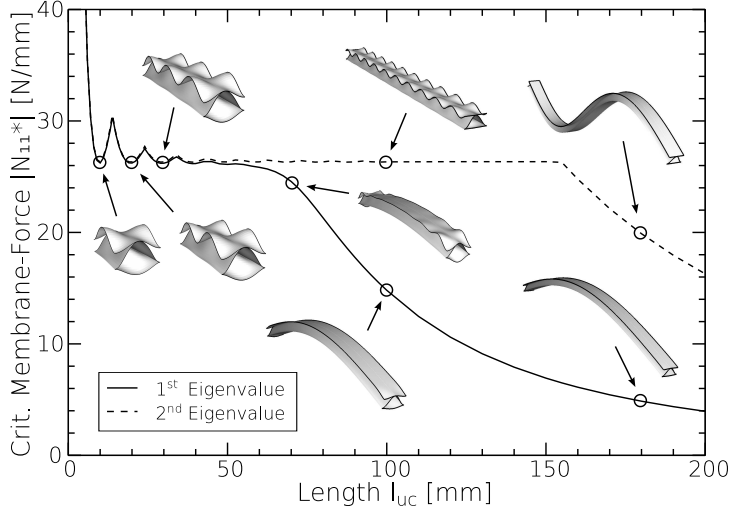


Figure 4: Systematic variation of the unit cell length l_{uc} and its effect on the critical compressive membrane force $|N_{11}^*|$ in the 1-direction.

in the present study only insofar, as a necessary minimum bending stiffness B_1 is required during the optimization procedure.

For finding the first minimum of the relationship $|N_{11}^*|(l_{uc})$ a one-dimensional optimization algorithm was sufficient. The Python package for scientific programming ‘SciPy’ [11] was used to set up the corresponding programming environment. SciPy offers an implementation of Brent’s method ([12]) in the form of the function ‘fminbound’ that was called for finding the unit cell length that corresponds to the wavelength of the buckling pattern of the infinite corrugated board strip.

The numerical scheme for the determination of the buckling membrane load in the longitudinal direction $|N_{11}^*|$ for a given set of governing geometrical parameters was then embedded into an optimization scheme for the minimization of the specific cross-sectional area \bar{A} . This scheme uses the SciPy function ‘fmin_cobyla’ for the determination of a local minimum for a given nonlinear objective function in the presence of nonlinear optimization constraints. ‘COBYLA’ is an acronym for ‘constrained optimization by linear approximation’. The corresponding iterative algorithm, that allows for an optimization without having to calculate derivatives, was originally proposed by Powell [13].

The stiffness constraint $B_1 \geq B_{1,0}$ was taken into account based on purely geometrical terms, namely the width-specific area moments of inertia of liners and fluting and their corresponding elastic moduli. It would certainly have been possible to calculate the effective stiffness of a given corrugated board by means of the available finite element unit cell, but in the light of the hundreds of simulation runs necessary to perform a complete optimization this was regarded as infeasible. Additionally, the accuracy of the analytical prediction proved to be high enough for all practical purposes.

With the described nested numerical optimization scheme it was possible to improve any given set of initial geometrical parameters in terms of the effective area-specific board weight while, at the same time, providing a corrugated board design with the necessary strength for avoiding local and global buckling.

3. Results

For the optimization of the reference configuration for isotropic material behavior, two approaches were proposed: a semi-analytical and a numerical one. The semi-analytical optimization method relied on an approximation of the buckling membrane force $|N_{11}^*|$ by means of a nonlinear fitting function. The optimization procedure could be formulated entirely within the software *Mathematica*.

Applying this method to the isotropic reference configuration (see Tab. 2, left) gives a result that

Table 2: Geometrical parameters of the isotropic reference configuration (*left*), the result of the semi-analytical optimization (*middle*) and the result of a subsequent numerical optimization (*right*).

Reference Configuration (isotrop)	Optimized Configuration (semi-analytical)	Optimized Configuration (numerical)
$b_{w1} = 7.2$ mm	$b_{w1} = 5.030$ mm	$b_{w1} = 4.830$ mm
$h_{uc} = 3.6$ mm	$h_{uc} = 4.230$ mm	$h_{uc} = 4.200$ mm
$t_L = 0.2$ mm	$t_L = 0.150$ mm	$t_L = 0.152$ mm
$t_F = 0.2$ mm	$t_F = 0.136$ mm	$t_F = 0.136$ mm
$\bar{A} = 0.6922$ mm	$\bar{A} = 0.5752$ mm	$\bar{A} = 0.5851$ mm

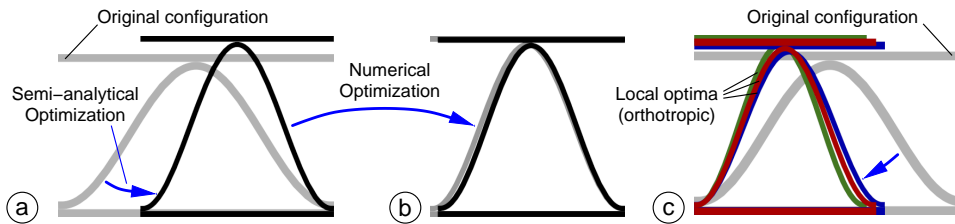


Figure 5: (a) Plot of the original configuration (gray) with the geometry resulting from the semi-analytical optimization for isotropic material behavior being superimposed in black color; (b) the previous result (gray) subjected to the numerical optimization procedure gives the geometry drawn in black. (c) Original configuration and the best three designs for orthotropic material behavior.

is 16.9% lighter than the reference configuration while predicting the same critical membrane force $|N_{11}^*| = |N_{11,0}^*|$ and the same bending stiffness $B_1 = B_{1,0}$, respectively, as the reference configuration, thus indicating a successful optimization procedure. The respective geometrical parameters are given in Tab. 2, *middle*). Corresponding cross-sections through the corrugated board are visualized in Fig. 5 (a). This figure shows that the thickness h_{uc} of the board increases as a result of the optimization procedure while the wavelength of the flute b_{w1} decreases. Therefore, the flanks of the sinusoidal flute become steeper. Both the thickness of the fluting paper and the thickness of the liners are reduced, which is the primary reason for the weight decrease.

It is now possible to use the result of the semi-analytical optimization as the initial configuration for a subsequent numerical optimization which uses an accurate finite element prediction of $|N_{11}^*|$ instead of the approximation with a fitting function used in the semi-analytical approach. The result, which is given in Tab. 2, *right*), is very promising insofar, as the geometrical parameters change only very little relative to the semi-analytical optimum. The value that is affected the most by the numerical optimization is the width b_{w1} , whereas the thickness of the fluting paper t_F does not change at all. Fig. 5 (b) visually demonstrates the similarity of the results.

Again, the weight per projected area was reduced compared to the original configuration, this time by 15.5%. Now it may appear surprising that the numerical optimization produces a design that is actually heavier than the semi-analytical one. The reason for this unexpected result can be found in the approximative nature of the prediction of $|N_{11}^*|$ in the semi-analytical approach, because the actual critical membrane force calculated with a finite element model having the geometry described in Tab. 2, *middle*) is 8.4% lower than the required buckling strength of $|N_{11,0}^*|$. In other words, the semi-analytical approach slightly overestimates the buckling resistance for the investigated case, leading to a design that is 1.7% lighter than the one proposed by the more accurate numerical method. Nevertheless, the similarity between the two designs is remarkable.

In the previous paragraphs the attribute ‘optimal’ has to be understood in a local sense. This can be demonstrated by using the isotropic reference configuration as the starting point for the numerical optimization instead of the semi-analytical optimum. This change gives a local optimum which is

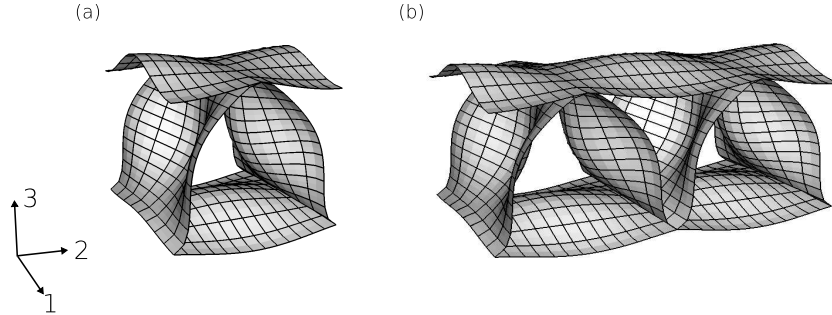


Figure 6: Simultaneous buckling of flute and liners in an optimized orthotropic corrugated board. In the considered case, the symmetry of the buckling mode with respect to the wavelength of the flute is maintained even if the unit cell width would allow for antisymmetric buckling modes (*right*).

slightly worse ($\bar{A} = 0.5856$ mm instead of 0.5851 mm) compared to the previously reported design. Furthermore, the COBYLA algorithm requires 109 iterations for achieving convergence as opposed to the 43 iterations necessary for achieving convergence when the semi-analytical optimum is the starting point of the numerical optimization. This indicates, that — due to the non-linearities involved — the starting configuration has an influence on the optimization result, indicating the existence of many local optima, and also affects the rate of convergence of the optimization algorithm. One has to keep in mind that for each iteration of the COBYLA algorithm the iterative calculation of $|N_{11}^*|$ consumes on the order of 10 individual finite element buckling analyses.

For the corrugated board design with orthotropic material behavior of fluting and liners very similar results were obtained. The initial configuration was documented in Tab. 1. Starting the COBYLA algorithm from this configuration gives an optimized design with $b_{wl} = 5.05$ mm, $h_{uc} = 4.04$ mm, $t_L = 0.208$ mm, and $t_F = 0.136$ mm. Again, the paper thicknesses were reduced, the overall board thickness was increased, and the flanks of the sinusoidal flute became steeper. The specific area \bar{A} was reduced to 0.6795, which means a weight reduction of 18.2%.

For the orthotropic board a systematic variation of the starting parameters was performed in order to investigate the existence of local optima in more detail. To this end, the following boundaries for the geometrical parameters were prescribed: $2.50 \leq b_{wl} \leq 10.0$, $2.00 \leq h_{uc} \leq 8.0$, $0.14 \leq t_L \leq 0.31$, and $0.09 \leq t_F \leq 0.21$, with all values being given in [mm]. Then, 16 optimization runs were performed with starting values for the geometric variables that were permutations of the boundary values given above. A geometrical interpretation of the different starting configurations can be given in terms of the corners of a hypercube in the 4-dimensional parameter space of the problem. The completion of the 16 optimization runs took 1780 COBYLA iterations and around 16000 finite element analyses in total. Only one set of initial parameters, namely $b_{wl} = 10$ mm, $h_{uc} = 8$ mm, $t_L = 0.14$ mm, and $t_F = 0.21$ mm, produced an optimized configuration ($b_{wl} = 4.82$ mm, $h_{uc} = 4.13$ mm, $t_L = 0.195$ mm, and $t_F = 0.141$ mm) that gave a more favorable \bar{A} of 0.6794 mm than the design originating from the reference configuration. The negligible difference in the specific weight indicates that conventional corrugated board designs may be good starting points for the described optimization procedure. It has to be added that none of the 16 starting configurations produced an optimized result for which any of the optimization variables assumed their respective boundary values. Fig. 5 (c) shows the three best designs obtained for the board with orthotropic material properties.

Looking at the buckling modes of the numerically optimized corrugated board designs yields additional insight into potential attributes of such optimized structures. Figure 6 shows the local buckling mode for the optimized configuration with orthotropic paper properties. Figure 6 (*left*) shows simultaneous buckling of fluting and liners, which supports the assumption of a simultaneous-buckling optimization criterion in the semi-analytical approach.

Furthermore, additional buckling analyses performed with finite element unit cell models of optimized configurations, that contained two full fluting waves, compare Fig. 6 (*right*), demonstrated, that in the

considered case the liners indeed buckle like clamped plates, i.e., symmetrical with respect to the bonding lines between fluting and liners. This indicates consistency of the optimized designs with the clamped boundary condition assumption inherent in the semi-analytical model and the finite element models that use only one full fluting wave over their width.

5. Conclusions

A scheme for the reduction of the area-specific weight of corrugated board by means of numerical optimization methods has been proposed. Strength constraints were implemented in terms of a required minimum resistance of the board against local and global elastic buckling. The former buckling mechanism could be quantified in closed form by semi-analytical approaches in the case of isotropic material behavior and by finite element unit cell buckling analyses in the case of orthotropic material behavior. Global elastic buckling was related to the effective bending stiffness about the axis transverse to the flute orientation with a corresponding required minimum value.

Numerical optimization schemes were then used to produce improved corrugated board designs by iteratively changing the principal geometrical parameters of the corrugated board in the sense of a sizing optimization. Compared to reference geometries a 15.5% weight reduction was achieved for the board made from isotropic material and a 18.2% weight reduction was achieved for the board made from orthotropic material. In both cases the resulting designs showed simultaneous buckling of liners and fluting under compressive membrane loads in the longitudinal direction indicating that this behavior may be characteristic of optimal solutions. While the non-linear nature of the optimization problem does not ensure the prediction of a true optimum in the strict, global sense, the applied algorithms proved to be robust and useful for improving given corrugated board configurations in terms of a reduction of their specific weight.

References

- [1] P. Patel, T. Nordstrand, and L. A. Carlsson. *Compos. Struct.*, 39(1–2):93–110, 1997.
- [2] U. Nyman and P. J. Gustafsson. *Compos. Struct.*, 50:79–83, 2000.
- [3] U. Nyman. *Continuum Mechanics Modelling of Corrugated Board*. PhD thesis, Lund University, Lund, Sweden, April 2004.
- [4] A. Allansson and B. Svärd. Stability and collapse of corrugated boards; numerical and experimental analysis. Master’s dissertation, Lund University, Lund, Sweden, 2001.
- [5] R. C. McKee, J. W. Gander, and J. R. Wachuta. *Paperboard Packaging*, 48(8):149–159, 1963.
- [6] M. E. Biancolini and C. Brutti. *Pack. Tech. Sci.*, 16:47–60, 2003.
- [7] T. Nordstrand. *Basic Testing and Strength Design of Corrugated Board and Containers*. PhD thesis, Lund University, Lund, Sweden, February 2003.
- [8] T. J. Lu, C. Chen, and G. Zhu. *J. Comp. Mat.*, 35(23):2098–2126, 2001.
- [9] T. Flatscher. Modellierung der Steifigkeit und Stabilität von Wellpappe. Diploma thesis, Vienna University of Technology, Vienna, 2006.
- [10] D. H. Pahr and F. G. Rammerstorfer. *CMES - Comp. Model. Eng.*, 12(3):229–242, 2006.
- [11] E. Jones, T. Oliphant, P. Peterson, et al. SciPy: Open source scientific tools for Python, 2001–.
- [12] R. P. Brent. *Algorithms for Minimization Without Derivatives*, chapter 3–4. Prentice-Hall, Englewood Cliffs, NJ, 1973.
- [13] M. J. D. Powell. In S. Gomez and J. P. Hennart, editors, *Advances in Optimization and Numerical Analysis*, pages 51–67. Kluwer Academic Publishers, Dordrecht, 1994.